



Stoichiometry control of magnetron sputtered $\text{Bi}_2\text{Sr}_2\text{Ca}_{1-x}\text{Y}_x\text{Cu}_2\text{O}_y$ ($0 \leq x \leq 0.5$) thin film, composition spread libraries: Substrate bias and gas density factors

R.J. Sanderson, K.C. Hewitt *

Department of Physics and Atmospheric Science, Dalhousie University, 6300 Coburg Road, Halifax, NS, Canada B3H 3J5

Received 15 April 2005; accepted 3 June 2005

Available online 15 July 2005

Abstract

A magnetron sputtering method for the production of thin-film libraries with a spatially varying composition, x , in $\text{Bi}_2\text{Sr}_2\text{Ca}_{1-x}\text{Y}_x\text{Cu}_2\text{O}_y$ ($0 \leq x \leq 0.5$) has been developed. Two targets with a composition of $\text{Bi}_2\text{Sr}_2\text{YCu}_2\text{O}_{8.5+\delta}$ and $\text{Bi}_2\text{Sr}_2\text{CaCu}_2\text{O}_{8+\delta}$ are co-sputtered with appropriate masks. The target masks produce a linear variation in opposite, but co-linear radial direction, and the rotation speed of the substrate table is sufficient to intimately mix the atoms. EDS/WDS composition studies of the films show a depletion of Sr and Bi that is due to oxygen anion resputtering. The depletion is most pronounced at the centre of the film (i.e. on-axis with the target) and falls off symmetrically to either side of the 75 mm substrate. At either edge of the film the stoichiometry matches the desired ratios. Using a 12 mTorr process gas of argon and oxygen in a 2:1 ratio, the strontium depletion is corrected. The bismuth depletion is eliminated by employing a rotating carbon brush apparatus which supplies a -20 V DC bias to the sample substrate. The negative substrate bias has been used successfully with an increased chamber pressure to eliminate the resputtering effect across the film. The result is a thin film composition spread library with the desired stoichiometry.

© 2005 Elsevier B.V. All rights reserved.

PACS: 74.72.-h; 74.72.Hs; 74.78.Bz

Keywords: High- T_c films; Bi-based cuprates; Cuprate superconductors (high- T_c and insulating parent compound); Composition spread libraries; Magnetron sputtering; Stoichiometry; Resputtering; Substrate bias

1. Introduction

It is widely accepted that oxygen has to be added to the sputtering gas for the deposition of $\text{Bi}_2\text{Sr}_2\text{CaCu}_2\text{O}_{8+\delta}$ (Bi-Ca-2212) thin films [1–4].

* Corresponding author. Tel.: +1 902 4942315; fax: +1 902 4945191.

E-mail address: kevin.hewitt@dal.ca (K.C. Hewitt).

URL: <http://fizz.phys.dal.ca/~hewitt> (K.C. Hewitt).

The drawback to using oxygen in the sputtering gas is a pronounced resputtering of the deposited film, as found in Bi-Ca-2212 [5,6] and $\text{YBa}_2\text{Cu}_3\text{O}_{7-\delta}$ [7–11] superconducting systems. Oxygen anions derived from the sputtering gas and target material are the source of this resputtering effect [12]. The anion is accelerated away from the negatively charged target, and if the energy is large enough, it will escape the magnetron's magnetic field. The energetic anions sputter the deposited film, in a manner that preferentially depletes atoms with large scattering cross-sections. This resputtering effect produces the undesirable effect of changing the composition of the film relative to the target.

There have been several reported methods to reduce the resputtering phenomenon in these materials. The most common approach is to use an off-axis deposition method, where the substrate is not directly across from the target. Rather, the substrate is placed at an angle $<90^\circ$ relative to the axis of the cylindrical target. It has been found that the energy of oxygen anions that strike the film is reduced [1,5–11]. Off-axis sputtering greatly reduces the deposition rate, which is not desirable. To further reduce resputtering, it has been shown that increasing the sputtering gas pressure can increase the anion-gas collisions, reducing their energy or deflecting them away from the film. Increasing the gas pressure usually reduces the target bias. The energy of the anions is thereby decreased; however, the increased gas pressure also decreases the film deposition rate due to target atom-gas collisions. A third method to compensate for resputtering is to alter the target stoichiometry to account for the non-uniform depletion of elements [5,7,9]; this is sometimes not possible as the required target composition may not be an equilibrium phase. A final method uses a negative bias shield or substrate bias to deflect the anions away from the deposited film [1,3].

Physical vapor deposition has been used since 1965 to explore phase diagrams using a composition-spread approach [13–18]. In this technique, a large range of compositions is deposited on a single substrate in a single deposition run. Our group has established a composition spread approach which uses magnetron sputtering to prepare a con-

tinuous variation of composition across a 75 mm substrate [19].

Therefore, to develop a magnetron sputtering method for the production of cuprate superconductor thin-film samples with a spatially varying composition, x , in $\text{Bi}_2\text{Sr}_2\text{Ca}_{1-x}\text{Y}_x\text{Cu}_2\text{O}_y$ ($0 \leq x \leq 0.5$), resputtering effects have to be addressed as it has a detrimental effect on the composition of the deposited film. An apparatus had to be designed to bias the substrates while affixed to a rotating substrate table. The novel aspect of this paper is the introduction of a rotation-compatible substrate bias apparatus that uses an existing magnetron to supply a constant -20 V bias to the substrates in order to prepare a cuprate superconductor composition spread library.

2. Experiment and results

The composition spread approach uses simultaneous, magnetron sputtering of two targets, e.g. A and B. Masks are placed over each target to produce a linear variation in the mass deposited onto a water-cooled, rotating substrate as described in more detail in reference [19]. When the linear variation is in opposite, but co-linear radial direction, and the rotation speed (15 revolutions per minute) is sufficient to intimately mix the atoms, a film A_{1-x}B_x ($0 \leq x \leq 1$) is produced radially across a 7.5 cm doughnut on a 43 cm diameter substrate table—the doughnut is centered at a radius of 13.5 cm from the substrate centre. To produce a film $\text{Bi}_2\text{Sr}_2\text{Ca}_{1-x}\text{Y}_x\text{Cu}_2\text{O}_y$ ($0 \leq x \leq 1$), one must therefore co-sputter two targets: A = $\text{Bi}_2\text{Sr}_2\text{CaCu}_2\text{O}_{8+\delta}$ (Bi-Ca-2212) and B = $\text{Bi}_2\text{Sr}_2\text{YCu}_2\text{O}_{8.5+\delta}$ (Bi-Y-2212).

The powders used to synthesize the targets are made through the same three-stage solid-state reaction sequence. To synthesize Bi-Ca-2212, powders of Bi_2O_3 (99.975%, Alfa-Aesar), SrCO_3 (99.99%, Alfa-Aesar), CaO (99.95%, Alfa-Aesar) and CuO (99.7%, Alfa-Aesar) are measured in the appropriate stoichiometric ratios and ground together for two hours using an agate auto grinder. The mixture is first reacted in air at 800°C for 12 h (slow heat/slow cool at $4^\circ\text{C}/\text{min}$), to calcinate the powders. After the first reaction, the

powder is ground for 2 h. The next two reactions in air are at 870 °C. Between these two 870 °C reactions the powder is ground for 2 h. To produce Bi-Y-2212, Y₂O₃ (99.9%, Alfa-Aesar) is used instead of CaO. Once the target powders are synthesized, they are pressed into pucks and hardened before use. To accomplish this, the powder is ground manually with an agate mortar and pestle and sifted through a 70 μm sieve. Next, approximately 40 g of the sieved powder is pressed into a 5.08 cm (2 in.) diameter by 0.5 cm thick disc using a pressure of 8500 psi. The disc is sintered to harden the target and reduce porosity. The sintering temperature was chosen to be close to the melting temperature for each of the two targets (Bi-Ca-2212—875 °C and Bi-Y-2212—935 °C).

Fig. 1 shows X-ray spectra of the Bi-Ca-2212 and Bi-Y-2212 target materials collected with a Siemens D500 X-ray spectrometer using CuK_α X-rays. Using the Bbmb(D_{2h}²⁰) space group (non-conventional setting of Cccm), the powder X-ray spectrum for each target was fit with Rietica V1.62—a Rietveld analysis program. Fig. 1 shows the X-ray diffraction spectra, as well as the fit for each material, and Tables 1 and 2 shows the refined parameters. The fits to the spectra demonstrate that the space group Bbmb is a reasonable choice for the Bi-2212 phase. Goodness of fit (GOF) values for the Bi-Ca-2212 fit of 5.32 and 7.28 for the Bi-Y-2212 system are large. This large GOF is due to the fact that the orthorhombic space group is well known to represent an average

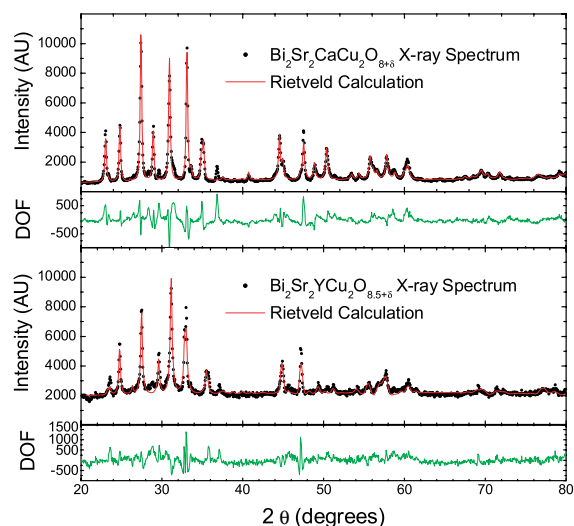


Fig. 1. Rietica analysis fit of the XRD patterns of Bi-Y-2212 and Bi-Ca-2212 target materials. DOF stands for difference of fit.

structure which does not account for the incommensurate modulation along the *b*-axis of 4.7*b*.

The change in unit cell size is consistent with previous reports [20]: the *a*-axis lattice parameter expands from 5.41 Å to 5.46 Å, *b*-axis lattice parameter expands from 5.40 Å to 5.43 Å and *c*-axis lattice parameter contracts from 30.80 Å to 30.18 Å. Overall, the volume contracts by 0.6% upon substitution of Y for Ca in accordance with previous reports which find a volume reduction of 0.7% [20].

Table 1

Rietica fit parameters for Bi-Ca-2212 (Bi/Sr means Bi in Sr sites and Ca/Sr means Ca in Sr sites)

Space group: Bbmb(D _{2h} ²⁰)				
<i>a</i> = 5.405(3) Å,		<i>b</i> = 5.402(2) Å,	<i>c</i> = 30.804(2) Å	
Goodness of fit: 5.32				
Atom	<i>x</i>	<i>y</i>	<i>z</i>	Occ.
Bi	0.5	0.515(2)	0.2425(1)	1.05(7)
Sr	0.0	0.1394(6)	0.2448(3)	0.91(1)
Ca	0.0	0.25	0.25	0.91(1)
Cu	0.5	0.1947(4)	0.2370(5)	1.04(7)
Bi/Sr	0.0	0.1394(6)	0.2448(3)	0.053(4)
Ca/Sr	0.0	0.1394(6)	0.2448(3)	0.036(1)
O(1)	0.0	0.1695(7)	0.057(9)	1.7(5)
O(2)	0.25	0.1193(1)	0.2974(3)	1.1(1)
O(3)	0.0	0.0287(5)	0.1374(4)	0.5(8)

Table 2
Rietica fit parameters for Bi-Y-2212

Space group: Bbmb(D_{2h}^{20})				
$a = 5.45(9) \text{ \AA}$,		$b = 5.428(5) \text{ \AA}$,	$c = 30.185(2) \text{ \AA}$	
Goodness of fit: 7.28				
Atom	x	y	z	Occ.
Bi	0.5	0.503(9)	0.2763(1)	0.88(0)
Sr	0.0	0.1354(4)	0.2444(3)	1.34(1)
Y	0.0	0.25	0.25	0.6882(6)
Cu	0.5	0.195(8)	0.232(2)	0.7293(4)
O(1)	0.0	0.152695(7)	0.0	1.328(8)
O(2)	0.25	0.1892(2)	0.5	1.8(9)
O(3)	0.5	0.1605(6)	0.2801(4)	1.2(6)

To confirm the electrical properties of each material, low temperature resistance measurements were made. Each target material was pressed into a 1.2 cm diameter \times 0.5 cm pellet and sintered. Silver contact pads were evaporated onto the pellet to improve conduction to the sample. Four Cu wires were affixed with silver epoxy to the pellet on top of the silver pads, to perform a 4-probe resistance measurement. The pellets were mounted into a Janis CCS-450 cold helium gas compressor cryostat system, and cooled as a constant current of 100 mA was applied and the subsequent voltage measured. Using V/I , the resistance versus temperature plots for the two materials are shown in Fig. 2. It can be clearly seen that the Bi-Y-2212 material behaves as an insulator, while the Bi-Ca-2212 material shows a $T_{c,onset} \approx 67 \text{ K}$.

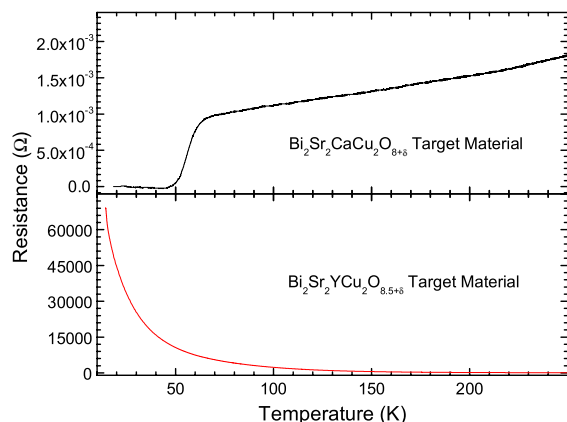


Fig. 2. Low temperature four-probe resistance measurements of Bi-Y-2212 and Bi-Ca-2212 target materials.

The film deposition apparatus is a Corona Vacuum Coaters V-37 sputtering system equipped with 5 magnetrons configured in a side-sputtering arrangement, where the substrate is directly across (5.5 cm) from the target. To power the magnetrons either an Advanced Energy MDX-1 K DC supply or a combination of an Advanced Energy RFX-600 generator and RTX-600 tuner is chosen for the Bi-Ca-2212 (conductor) and Bi-Y-2212 (insulator) targets, respectively. Typical sputtering conditions are shown in Table 3. Energy dispersive spectroscopy (EDS) measurements were made using a JEOL JXA-8200 Superprobe equipped with a Noran energy detector (0.133 keV energy resolution). A 15 kV electron beam with a 20 nA current is used to analyze a 10 μm spot. The film is deposited onto polished Al or Si-wafer substrates for composition analysis. Polished Al was chosen due to partial X-ray peak overlap between the K_{α} and K_{β} X-rays of Si (1.74 and 1.83 keV, respectively) and the L_{α} and L_{β} X-rays of Sr (1.81 and 1.87 keV, respectively). Polished Si wafers provide a better surface for determination of Bi, Ca and Cu. In addition, the film is deposited onto single crystal (100) MgO substrates, through a slotted aluminum mask (0.5 mm slots separated

Table 3
Typical sputtering conditions

Target	Bi-Ca-2212	Bi-Y-2212
Sputtering power	70 W DC	109 W RF
Base pressure (Torr)		4.0×10^{-7}
Deposition time		60 h
Deposition thickness		1.2 μm

by 1.5 mm across the 75 mm substrate), for post-annealing studies.

For all deposited films, X-ray diffraction (XRD) spectra were collected using an Inel CPS-120 with a curved position sensitive detector. The $\text{CuK}_{\alpha 1,2}$ X-ray beam is incident upon the sample at approximately 6° and the curved position sensitive detector collects all scattered X-rays from $2\theta = 3$ to 119° . Collection time for the XRD spectra was typically 1800 s. The Inel and the JEOL both have computer controlled sample stages to scan samples precisely and efficiently.

Using energy dispersion spectroscopy (EDS) the normalized composition of Bi and Sr across the deposited film from three runs is shown in Fig. 3. Panels A, B and C correspond to sputtering conditions as listed in Table 4.

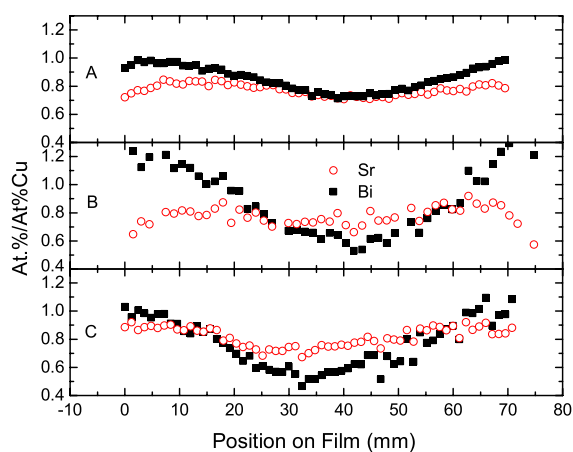


Fig. 3. EDS compositional analysis of Bi (filled square) and Sr (empty circle) as per position along the film. Data has been normalized to the atomic percent Cu present in the film. (A) SPI102, (B) SPJ098 and (C) SPI131.

Table 4

Sputtering gas conditions for results presented in Fig. 3

Fig. 3 panel	A (SPI102)	B (SPJ098)	C (SPI131)
Base pressure (Torr)	4.57×10^{-7}	4.92×10^{-7}	3.52×10^{-7}
Chamber pressure (Torr)	5.71×10^{-3}	12.0×10^{-3}	13.2×10^{-3}
O_2 :Ar flow rate (sccm)	2:4	5:10	1:13
O_2 :Ar ratio	1:2	1:2	1:13

The data shown in Fig. 3 illustrates the effect that both oxygen concentration and sputtering pressure have on resputtering. Panel A shows resputtering in both Bi (30% depletion at the center of film relative to edge) and Sr (13% depletion at the center of film relative to edge) with a 1:2 = O_2 :Ar ratio. Panel B shows there is reduced resputtering of Sr (<1%) as the O_2 :Ar ratio is kept constant, but the pressure increased. However, as seen in the data of panel B, Bi is still resputtered (42% depletion at the center of film relative to edge). Panel C shows the data collected from a sputtering run with the working pressure comparable to panel B, but the O_2 :Ar ratio decreased to 1:13. The degree of resputtering is comparable to that which is present in panel B (40% depletion at the center of film relative to edge), but there was significant damage to the Bi-Ca-2212 target. This damage may be due to oxygen depletion on the surface of the target, and has not been present in runs with increased O_2 :Ar ratios. Of the data presented in Fig. 3, panel B shows the most desirable characteristics.

Fig. 4 shows XRD spectra of the as-deposited films from the deposition that produced the composition shown in Fig. 3, panel B as a function of position along the film. The presence of broad peaks shows the amorphous nature of the films.

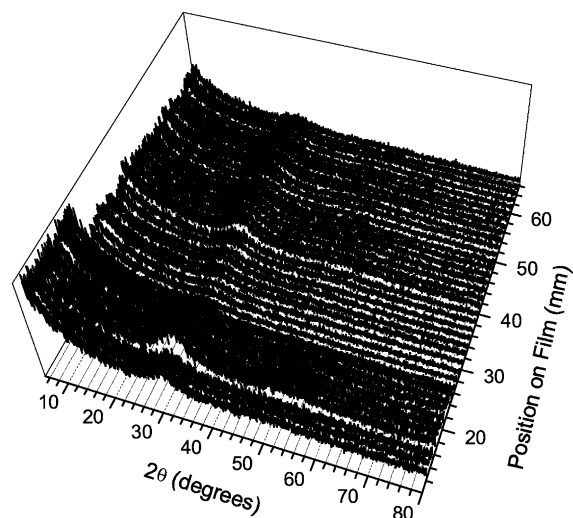


Fig. 4. XRD spectra of the as-deposited film (SPJ098) as a function of position along the substrate.

As such, the films must be annealed to crystallize the Bi-2212 phase.

The as-deposited film whose EDS data are shown in Fig. 3 (panel B) was post-annealed in a covered alumina crucible. According to Rubin et al. [21], the deposited films can develop Bi deficiency during annealing. To compensate, they added Bi_2O_3 powder to enrich the atmosphere with Bi, since Bi_2O_3 has a lower vapor pressure than the BiO in the films [21]. Adapting the annealing regime from Tsukamoto et al. [22] and using Rubin's suggestion, the films were annealed as follows. The furnace was heated to 780°C at which point the film, previously placed in a covered alumina crucible with powdered Bi_2O_3 , was inserted. The crucible was introduced to the furnace for 0.5 h, after which it was removed from the furnace and air quenched to room temperature. The furnace was then heated to 860°C and the samples were again inserted into the hot furnace for 6 h, and then removed.

X-ray diffraction patterns of the annealed film deposited on MgO are shown in Fig. 5. The XRD spectra reveal the presence of two major phases—the desired Bi-2212 phase and a second, more dominant, Bi_2SrO_4 phase. Fig. 6 shows the

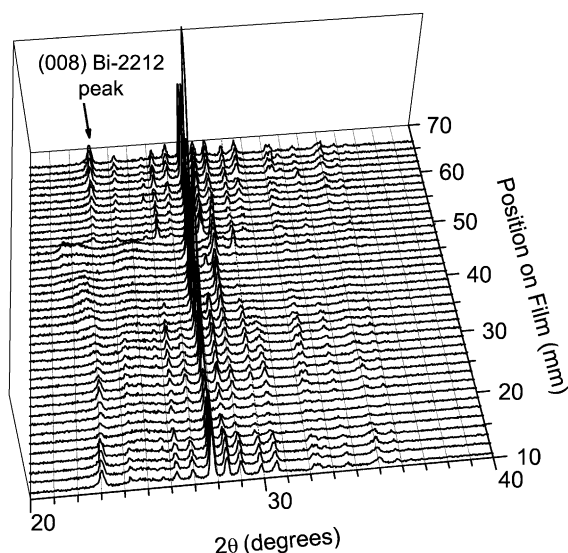


Fig. 5. XRD of the post-annealed film (SPJ098) as a function of position along the substrate. The (008) peak of the Bi-2212 structure is indicated by an arrow.

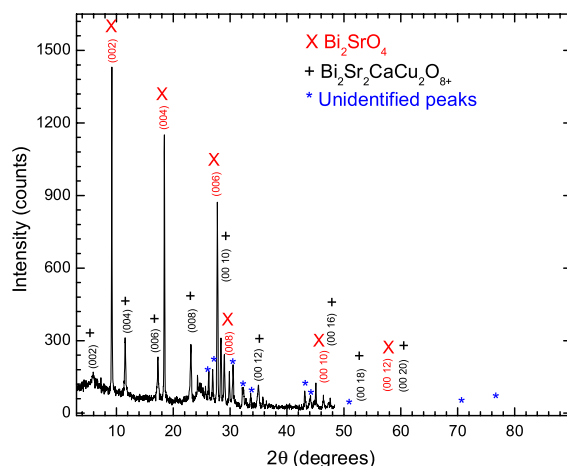


Fig. 6. XRD spectra of the post-annealed film (SPJ098) at a position of 10.4 mm (see Fig. 5). Shown are the (hkl) indices of the peaks of the two predominant phases, Bi_2SrO_4 and $\text{Bi}_2\text{Sr}_2\text{CaCu}_2\text{O}_{8+\delta}$.

XRD spectra corresponding to a point 10.4 mm from the inner edge of the film, and the (hkl) indices of the two phases. It is possible that the Bi_2SrO_4 phase is induced from the presence of Bi_2O_3 in the anneal atmosphere, though there is no firm evidence of this. Fig. 6 also reveals that the film exhibits epitaxial growth, since only $(hkl) = (00l)$ X-ray peaks are observed. Thus, the films are oriented with the c -axis perpendicular to the plane of

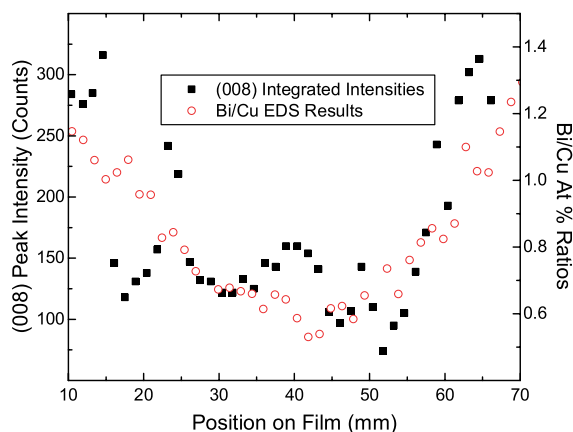


Fig. 7. Integrated intensity of the (008) Bi-2212 peak and EDS results from Fig. 3, panel B plotted as per position along the deposited film (SPJ098).

the substrate—a very desirable feature. The intensity of the (008) peak of the Bi-2212 phase diminishes as the film progresses toward the center, and begins to reappear and increase in intensity past the center.

Fig. 7 shows the correlation of (008) peak area with the Bi/Cu ratio as seen in Fig. 3, panel B. It is obvious that deposition of the correct Bi concentration is needed to create the desired Bi-2212 phase.

In an attempt to produce a pure Bi-2212 phase, a deposition was made with just the Bi-Ca-2212

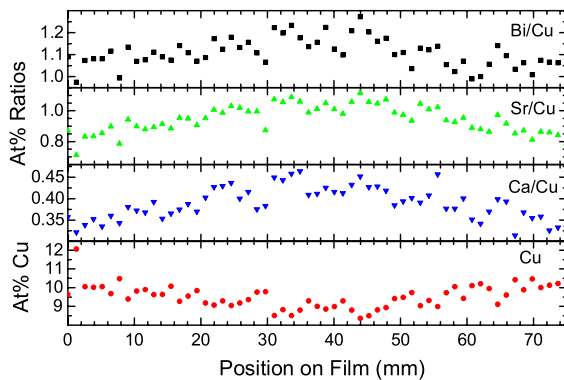


Fig. 8. EDS data of a Bi-Ca-2212 deposition (SPJ113). The peaks in the normalized atomic ratios is from the uncharacteristic depletion of Cu in the center of the film.

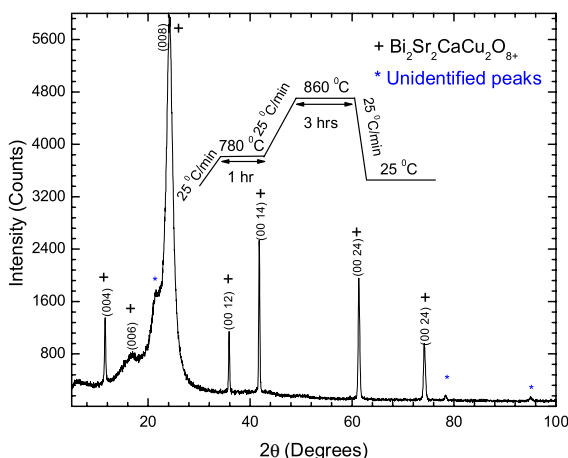


Fig. 9. XRD of a post-annealed film (SPJ113) segment (0–10 mm) from the deposition whose EDS results are shown in Fig. 8. The film was post-annealed as shown in the diagram.

target. This run was carried out with the same conditions as listed in Table 4. Single crystal (100) MgO substrates were placed on the edge of the film (over the last 10 mm of the sputtering track), without any physical masks. A film of approximately 1.5 μm was deposited. EDS of the film is shown in Fig. 8 where it is seen that the normalized data for Bi, Sr and Ca appear to have a peak in the center. Further inspection revealed an unexpected deficiency of Cu at the center which increases the normalized atomic ratio of Bi in the center. However, near the edges the stoichiometry matches the desired ratios. This problem with Cu deficiency has not resurfaced in numerous depositions.

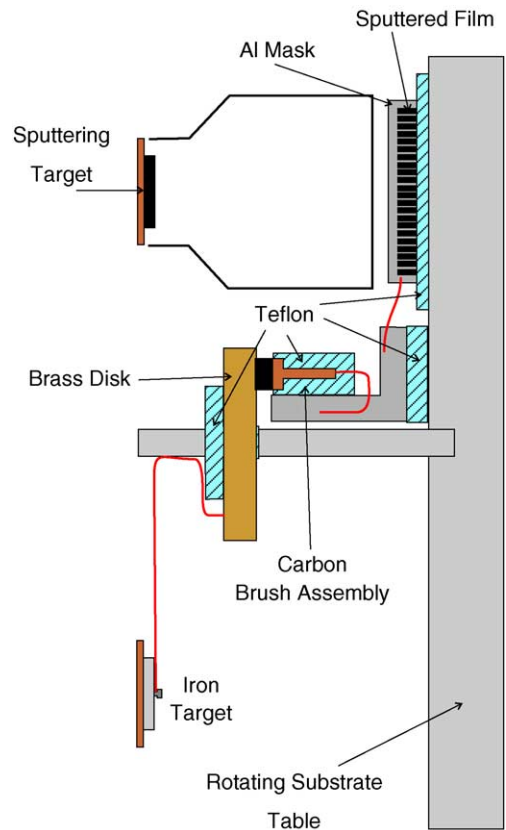


Fig. 10. Schematic of the rotating substrate bias apparatus. As the table rotates the carbon brush remains in contact with the brass disk that has been charged by an available magnetron. A bias of -20 V is applied to an Al mask to deflect the oxygen anions, and eliminate resputtering.

The film was subject to an annealing regime consisting of a quick ramp (25 °C/min) to 780 °C for one hour followed by a second identical quick ramp to 860 °C for three hours. As shown in Fig. 9 the result is a partially crystalline phase. The sharp peaks in the pattern were identified as (00*l*) peaks of the Bi-2212 phase (with two weak unidentified peaks). The (006) peak is broad demonstrating the partially amorphous nature of the annealed films. The film would have to undergo a longer anneal period to fully crystallize. However the lack of the Bi₂SrO₄ phase is reassuring.

Though the film composition at the edges are in the desired ratio and produce the desired phase, there is still a non-stoichiometric proportion of Bi near the centre of the film. To reduce this effect, a negative substrate bias had to be constructed to deflect oxygen anions away from the film. The film is deposited onto a rotating substrate. Thus one needs to design a rotating contact brush system. The substrates are either conductive, or have a conductive mask, consequently creating a substrate/mask bias is easily done, if an appropriate electrical contact system can be designed. Fig. 10 shows a schematic of a carbon brush assembly that

was manufactured on-site. It uses an existing magnetron to supply a negative bias to the substrate.

As the substrate table rotates, the carbon brush remains in contact with the brass disk. The brass disk is fixed to a central rod which is attached to the back of the sputtering chamber. An insulated wire electrically connects the brass disk to a 7 mm thick iron target. The iron target is thick enough so that the magnetic field from the magnetron is contained in the iron and only a small bias is applied, hindering the possibility of the formation of plasma and the subsequent sputtering of the iron. During deposition, a negative bias is applied to the iron target, and through the carbon brush assembly this bias is passed to the rotating substrate table. Using insulated wires the carbon brush assembly is connected to conductive Al masks (for MgO) or Al or Si substrates. Any negative bias can be applied by the magnetron, and in this case –20 V DC was chosen. The –20 V DC bias should be enough to reduce resputtering when teamed with an increased working pressure, but not high enough to induce any sputtering of the sample from any positive ions in the chamber. The brass disk, carbon brush assembly and the

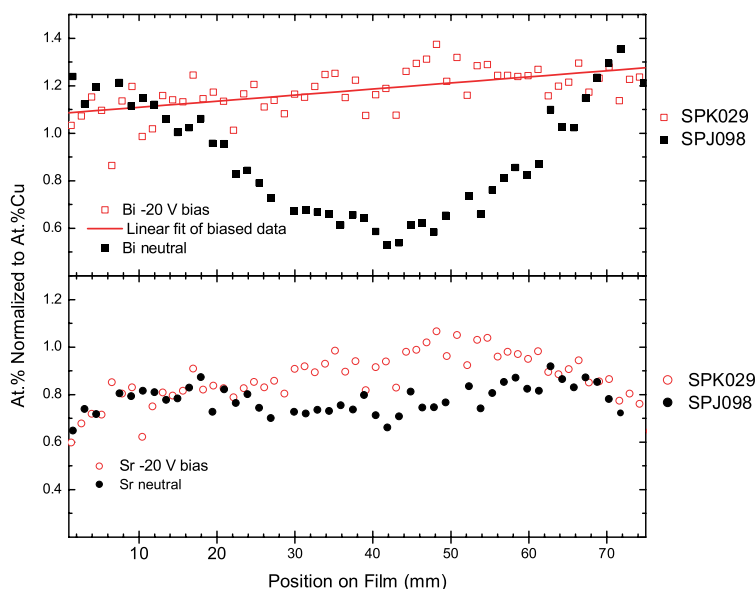


Fig. 11. EDS data from two sputtering runs carried out under identical sputtering conditions except that in one of the runs the aluminum substrate was charged with a –20 V DC bias (open symbols—SPK029) and in the other run the substrates were left neutral (filled symbols—SPJ098). Films deposited on polished Al substrates.

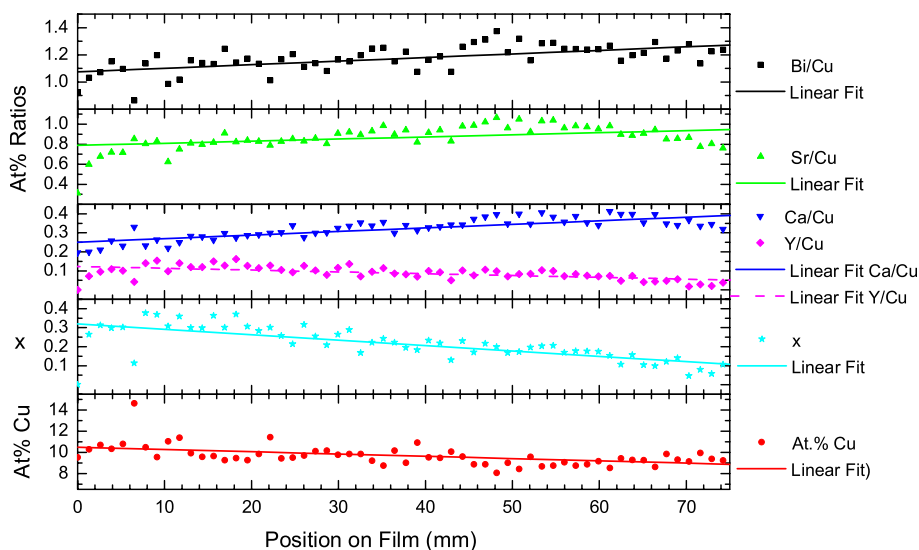


Fig. 12. EDS data from a run with both Bi-Y-2212 and Bi-Ca-2212 targets (SPK029). A -20 V substrate bias is used.

substrate are electrically insulated from the chamber by teflon insulators.

Fig. 11 shows EDS data for a $\text{Bi}_2\text{Sr}_2\text{Ca}_{1-x}\text{Y}_x\text{Cu}_2\text{O}_y$ ($0 < x < 0.4$) deposition using the rotating substrate bias apparatus with a bias of -20 V DC, and sputtered with similar conditions to column B in Table 4. The uniformity of the normalized Bi content across the biased sample demonstrates the effectiveness of the substrate bias to eliminate the resputtering effect. The similarities between the Sr content in both samples is also reassuring, in that the composition of the Sr was not greatly affected by the sample bias.

The complete as-deposited EDS profile for co-deposition of Bi-Y-2212 and the Bi-Ca-2212 targets with a -20 V substrate bias is shown in Fig. 12. The levels of Bi, Sr and Cu are relatively constant across the film, and the ratios of Bi and Sr are consistent with the stoichiometric ratios needed to form Bi-2212. For this deposition the physical mask on Bi-Ca-2212 was changed to produce a constant mass deposition across the film, while the Bi-Y-2212 target mask produced a linear gradient across the radius of the doughnut shaped sputtering track. The result is an amorphous film with the stoichiometric ratios needed to produce a set of $\text{Bi}_2\text{Sr}_2\text{Ca}_{1-x}\text{Y}_x\text{Cu}_2\text{O}_y$ films with $0.1 < x <$

0.4. Post-annealing studies of the as-deposited conducted under a variety of conditions will be reported in a subsequent paper.

3. Conclusions

Composition studies demonstrate the need for correct stoichiometry across the whole film for the formation of the Bi-2212 phase. Through the development of a rotating carbon brush apparatus, a -20 V DC bias can be applied to the sample substrate. The negative bias has been used successfully with an increased chamber pressure to reduce the resputtering effect across the film. Thus, with these methods, one may produce the desired stoichiometry in films prepared by the composition spread approach.

Acknowledgements

We would like to acknowledge valuable discussions with J.R. Dahn, A.E. George and S. Trussler. The financial support of the Natural Sciences and Engineering Research Council of Canada is gratefully acknowledged.

References

- [1] S.K. Park, J.H. Je, *Physica C* 245 (1995) 167.
- [2] R.H. Hammond, R. Borman, *Physica C* 162–164 (1989) 703.
- [3] A.C. Westerheim, L.S. Yu-Jahes, A.C. Anderson, *IEEE Trans. Magn.* 27 (1991) 101.
- [4] D.E. Morris, C.T. Hultgren, A.M. Markelz, J.Y.T. Wei, N.G. Asmar, J.H. Nickle, *Phys. Rev. B* 39 (1989) 6612.
- [5] J.M. Grace, D.B. McDonald, M.T. Reiten, J. Olson, R.T. Kampwirth, K.E. Gray, *J. Vac. Sci. Technol. A* 10 (1992) 1600.
- [6] J.M. Grace, D.B. McDonald, M.T. Reiten, J. Olson, R.T. Kampwirth, K.E. Gray, *J. Appl. Phys.* 70 (1991) 3867.
- [7] J.-H. Xu, G.-G. Zheng, A.M. Grishin, B.M. Moon, K.V. Rao, J. Moreland, *Appl. Phys. Lett.* 64 (1994) 1874.
- [8] S.S. Nathan, G. Mohan, S. Mohan, *Thin Solid Films* 347 (1999) 14.
- [9] C. Blue, P. Boolchand, *Appl. Phys. Lett.* 58 (1991) 2036.
- [10] P.H. Ballentine, J.P. Allen, A.M. Kadin, D.S. Mallory, *J. Vac. Sci. Technol. A* 9 (1991) 1118.
- [11] J.D. Klien, A. Yen, *J. Vac. Sci. Technol. A* 9 (1991) 1600.
- [12] J.J. Cuomo, R.J. Gambino, J.M.E. Harper, J.D. Kuptsis, J.C. Webber, *J. Vac. Sci. Technol.* 15 (1978) 281.
- [13] K. Kennedy, T. Stefansky, G. Davy, V.F. Zackay, E.R. Parker, *J. Appl. Phys.* 36 (1965) 3808.
- [14] J.J. Hanak, *J. Mater. Sci.* 5 (1970) 964.
- [15] X.D. Xiang, X. Sun, G. Briceno, Y. Lou, K.-A. Wang, H. Chang, W. Wallace-Freedman, S.-W. Chen, P. Schultz, *Science* 268 (1995) 1738.
- [16] R.B. van Dover, L.F. Schneemeyer, R.M. Fleming, *Nature* 162 (1998) 392.
- [17] H. Chang, I. Takeuchi, X.-D. Xiang, *Appl. Phys. Lett.* 74 (1999) 1165.
- [18] X.-D. Xiang, *Annu. Rev. Mater. Sci.* 29 (1999) 149.
- [19] J.R. Dahn, S. Trussler, T.D. Hatchard, A. Bonakdarpour, J.N. Mueller-Neuhaus, K.C. Hewitt, M. Fleischauer, *Chem. Mater.* 14 (2002) 3519.
- [20] I.-J. Hsu, R.-S. Liu, J.-M. Chen, R.-G. Liu, L.-Y. Jang, J.-F. Lee, K.D.M. Harris, *Chem. Mater.* 12 (2000) 1115.
- [21] L.M. Rubin, T.P. Orlando, J.B. Vander Sande, *Physica C* 220 (1994) 284.
- [22] K. Tsukamoto, H. Shimojima, M. Ishii, N. Enomoto, C. Yamagishi, *J. Am. Ceram. Soc.* 76 (1993) 1031.